

RECONSTRUCTION OF THE SUBSURFACE STRATIGRAPHY OF THE EXOMARS OXIA PLANUM LANDING SITE THROUGH INVESTIGATIONS OF EXPOSED BEDROCK WITHIN CRATER WALLS.

A. Srivastava^{1,2} L. L. Tornabene^{1,2} G. R. Osinski^{1,2}, C. M. Caudill³, P. Fawdon⁴, P. Grindrod⁵, E. Hauber⁶, J. Davis⁷, M. Pajola⁸, M. A. Soukup², V. G. Rangarajan^{1,2} ¹Department of Earth Sciences & ²Institute of Earth and Space Exploration, University of Western Ontario, London, ON, Canada. (asriva57@uwo.ca) ³Geomatics and Cartographic Research Centre, Carleton University, Ottawa, Canada. ⁴The Open University, Milton Keynes, UK. ⁵Natural History Museum, London, UK. ⁶DLR Institut für Planetenforschung, Berlin, Germany. ⁷Imperial College London, London, UK. ⁸INAF-Astronomical Observatory of Padova, Italy.

Introduction: The European Space Agency (ESA) is sending the next rover to Mars in 2028, named Rosalind Franklin, as part of the ExoMars mission. The main aim of the rover is to look for signatures of past aqueous activities on Mars that may have provided habitable environments for life. To meet these objectives, Oxia Planum was the chosen landing site for this rover because of its widespread Fe/Mg phyllosilicate exposures, ancient Noachian-aged rocks and strong evidence of prolonged fluvial activity [1-3].

Oxia Planum is a low-lying plain between Chryse Planitia and Arabia Terra, at the outlet of Coogoon Vallis [4-5]. It has witnessed at least two episodes of fluvial activity; one associated with the deposition /alteration to form the widespread clay unit and, the second, as evidenced by a remnant fluvial-deltaic fan deposit found on the outlet of Coogoon Vallis [6-7]. Based on HiRISE (High Resolution Imaging Science Experiment) colour-infrared observations, previous studies have reported two subunits of clays with a bluish (more ferrous-bearing) and orange (more ferric-bearing) appearance, wherein the orange subunit lies atop the blue subunit [3,9,10]. There is evidence of compositional differences between the two subunits that suggests varying post-deposition aqueous alteration or different detrital material provenance [9,11,12].

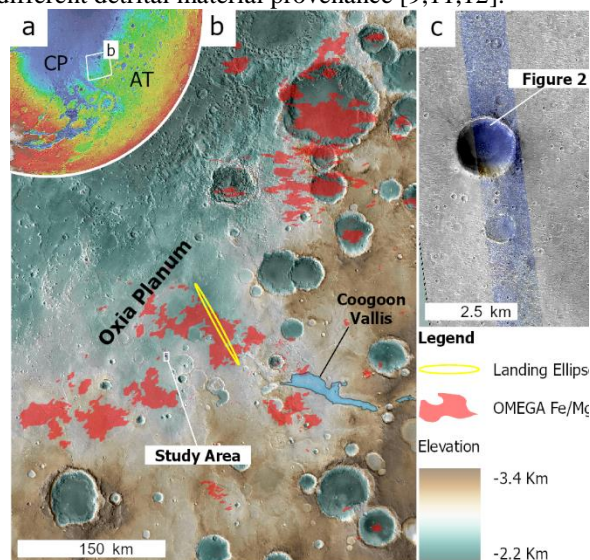


Fig. 1: the Context of this study (a) on Mars (b) with in Oxia Planum and (c) within ESP_073652_1980

Here we explore high resolution colour-infrared images of Oxia Planum crater walls, which, when fresh, would comprise impact ejecta overlying structurally uplifted target rocks [13-14]. These exposures may reveal the thickness and sequence of deposits representative of subsurface stratigraphy providing much more context for what is otherwise exposed at the surface and, through which, we hope to gain additional insights into the origins of the extensive clay-bearing units and history of Oxia Planum.

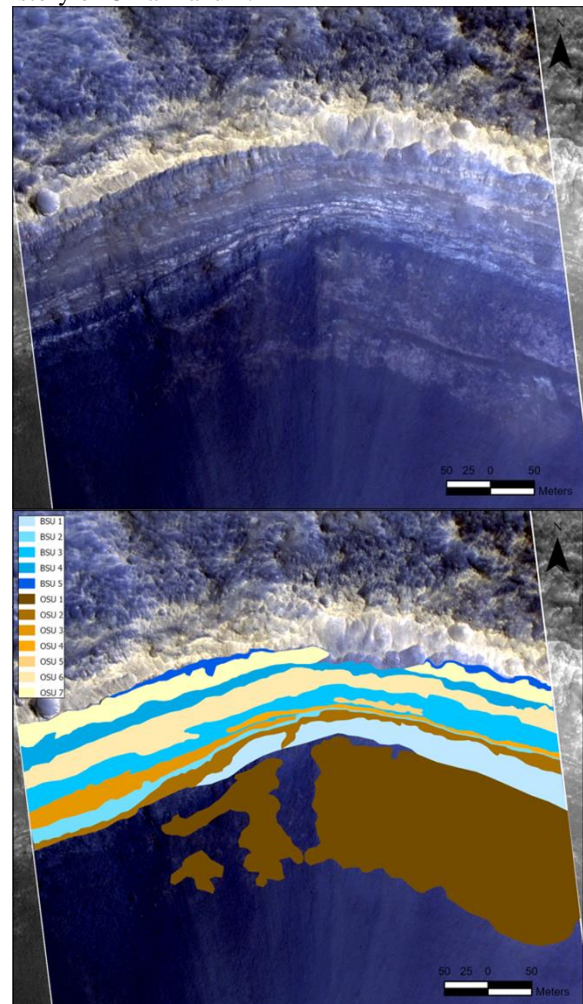


Fig. 2: (Top) HiRISE IRB image (ESP_073652_1980) of north crater wall overlaid on RED mosaic image. (Bottom) Map of north crater wall with individual orange subunits (OSU) and blue subunits (BSU) marked.

Methods: In this work, we focus on crater wall exposures of an unnamed crater southwest of the Oxia Planum landing site at 17.61 °N and 334.82 °E. (**Fig. 1**). Subsurface layers are observed to be very well-exposed on the north wall of this crater in a HiRISE colour-infrared (IRB) image (ESP_073652_1980) (**Fig. 2**). HiRISE is a multispectral push-broom imager with three bands (BG: blue-green, band center 536 nm; RED: panchromatic red band, band center 694 nm; and NIR: near-infrared, band center 874 nm) in the visible/near-infrared that provide colour sensitivity to ferric- and ferrous-bearing surface materials [15].

A Dark Subtraction (DS) correction was used to address time-variable scatter [16-18] after which we produced a Colour Band Ratio Composite (CBRC) with *IR/RED*, *RED/BG* and *RED/IR* in *R-G-B*, similar to [16]. The HiRISE CBRC was used to facilitate colour mapping because valid DS-corrected band ratios effectively reduce shading/illumination effects, thereby improving colour and spectral unit recognition [16-19]. Finally, ArcGIS Pro version 3.3 was used to map the extent of orange and blue subunits (OSU and BSU) by cross-referencing both HiRISE colour products.

Results: We mapped 5 BSUs and 7 OSUs using HiRISE IRB and CBRC images produced. The mapping is based on colour and texture differences between OSUs and BSUs. The individual OSU and BSU layers do not show many differences among them, and therefore, may not be compositionally different.

Discussion: Initial mapping results raise several interesting questions about the clay subunits, and the role of crater rim-formation with respect to what is observed within the wall exposure, and how they may relate to the subsurface target stratigraphy. The predicted stratigraphy in a well-preserved simple crater wall would be comprised of structurally uplifted target layers in its lower-most section, followed by an overturned “flap” of disaggregated, but relatively intact layers, and, finally, overlain by allochthonous impact breccias as part of the ballistic ejecta blanket. In addition, studies of terrestrial craters have also shown that crater rims are more structurally complicated than they seem with layers sometimes being ripped up and injected or wedged into/between other layers in the crater wall [14,20]. For example, OSU 5 may be one such wedge. BSU 2 and BSU 3 may also represent two merging beds, partially separated by a OSU 3 wedged in between them. Alternatively, some beds may be ripped apart during rim uplift, followed by overthrusting of layers making interpretations difficult.

While repetition of subunits raises the possibility of a potential overturned flap within the wall exposure, it is important to note that this only occurs in the very uppermost section of the exposure [20]. In theory, units

below the hinge line of the flap would be overturned and repeat. A possible interpretation is, therefore, that the hinge line of the overturned flap may be within OSU7 or BSU4, which would mean that BSU 4 and 5 and OSU 7 are all repeated subunits.

Regardless of the interpretation of the upper crater wall, the lower exposed section of the crater wall is still intriguingly comprised of multiple orange and blue subunits. Based on what is presently known about the stratigraphy of Oxia Planum, only one orange subunit is reported to be overlain by one blue subunit [3,9,10]. We consider two possible explanations for this. First, more than one orange and blue subunit may be present in this region, which also implies that blue subunit is not always on top of the orange as previously reported. Second, the subunits may in fact be interbedded as the evolution of the fluvial system, and its source materials, were likely to have evolved over time.

Conclusions: Our observations and mapping of several orange and blue subunits, infused with our understanding of terrestrial craters, indicate that the crater wall exposures may not be straightforward representations of target stratigraphy. Overall, the unique features of crater walls must be accounted for to accurately interpret the target stratigraphy. While ejecta and rim degradation may hamper defining these features, a pending HiRISE Digital Terrain Model (DTM) will hopefully aid in these identifications as well as help us to determine the thicknesses and orientations of the layers. Lastly, there are several other craters within the Oxia region whose crater walls are similarly well-exposed. These will need to be comparatively studied to see if a consistent subsurface target stratigraphy may be reconstructed and thereby improve our present understanding of the regional history.

References: [1] Carter J. et al. (2017) *Icarus*, 389. [2] McNeil J. D. et al. (2022) *JGR*, 127. [13] Quantin – Nataf C. et al. (2021) *Astrobiology*, 21. [4] Fawdon P. et al. (2021) *Journal of Maps*, 17(2). [5] Tanaka et al. (2014), *PSS*, 95. [6] Vago J. L. et al. (2017) *Astrobiology*, 17. [7] Brossier J. et al. (2022) *Icarus*, 386. [8] Fawdon P. et al. (2024) *Journal of Maps*, 20. [9] Mandon L. et al. (2021) *Astrobiology*, 21. [10] Parkes – Bowen A. et al. (2022) *PSS*, 214. [11] Gary-Bicas C. E. and Rogers A. D. (2021) *JGR*, 126. [12] Ivanov M. A. et al. (2020), *Solar System Research*, 54. [13] Melosh H. J. (1989) *Cambridge University Press*. [14] Sharpton V. L. (2014) *JGR*, 119. [15] McEwen A. S. et al. (2007) *JGR*, 112. [16] Tornabene L. L. et al. (2018) *SSR*, 214. [17] Rangarajan V. G. et al. (2023) *Icarus*, 115849. [18] Tornabene L. L. et al. (2023) *LPSC* 54, p.2727. [19] Dundas C. M. et al. (2023) *GRL*, 50. [20] Poelchau M. H. et al. (2009) *JGR*, 114.